Cosmological Information from Non-linear Weak Lensing

Zoltán Haiman

Xiuyuan Yang (Columbia)
Jan Kratochvil (Miami)

Other collaborators:
Morgan May (Brookhaven)
Eugene Lim (Cambridge)
Sheng Wang (Goldman Sachs)
Kevin Huffenberger (Miami)

KITP workshop on galaxy clusters UCSB 21 Apr 2011

Outline

- **Motivation:** is there significant information in the non-linear regime in WL beyond "usual" LSS statistics ?
    1. Statistical power of *dN/dz* (cluster counts)
    2. Complementarity of *dN/dz* and P_l (power spectrum)
- **Non-linear statistics robust to selection effects**:
    1. One-point function of convergence (analytic)
    2. Peak counts (including non-cluster peaks)
    3. Minkowski Functionals (V_0, V_1, V_2)

Motivation: Clusters

- **Exquisite statistical error forecast**

  from large SZ, XR, WL surveys – but have to know cluster mass M

- **“Phenomenological” self-calibration**

  e.g. $M=M_0(M/M_0)^{\alpha}(1+z)^{\beta}$ or more complicated forms

  use combination of mass-dependent observables dN/dz + P(k)

  (e.g. Majumdar & Mohr 2004; Wang et al. 2004)

- **“Physical” self-calibration**

  use parameterized cluster structure model to relate

  SZ, XR and WL observables (e.g. Shang, Haiman & Verde 2009; Younger et al. 2006)

- **WL surveys**

  200,000 (?!) clusters in 20,000 sq.deg. – problem: projections/selection

Motivation: WL surveys

- Several large (≳1,000 sq. deg) WL surveys forthcoming:

  (e.g. Pan-STARRS, KIDS, DES, LSST, Euclid)

- Shear power spectrum and related large-scale statistics

  (e.g. Kaiser 1992; Jain & Seljak 1997; Hu 1999, 2002; Huterer 2002; Refregier et al. 2004; Abazajian & Dodelson 2003; Takada & Jain 2004; Song & Knox 2004; ….)

  E.g. $\sigma(w_0)$=0.06; $\sigma(w_a)$=0.1 from 11-paramater fit to tomographic shear power spectrum (LSST) + *Planck*

- Comparable statistical errors from cluster number counts

  (e.g. Wang et al. 2004, 2005; Fang & Haiman 2007; Takada & Bridle 2007; Marian & Bernstein 2006, 2008)

  E.g. $\sigma(w_0)$=0.04; $\sigma(w_a)$=0.09 from 7-paramater fit to ~200,000 shear-selected cluster counts (LSST) + *Planck*

Motivation: Clusters vs Peaks

- Cluster counts and shear power spectrum can be considered independent observables – high synergy
  Covariance changes parameter-estimates by < few %
  (Fang & Haiman 2007; Takada & Bridle 2007)

- However, selection effects are (probably) a showstopper in a WL survey alone, due to projection effects
  Filter-dependent trade-off between *completeness* and *purity*: "best compromise" values are ~70% for both
  (e.g. White et al. 2002; Hamana et al. 2005; Hennawi & Spergel 2005)

- Why not define observable immune to projection effects?
  historical reason: cosmology-dependence of halo mass function calculable from "Press-Schechter"

Peak counts

- A simple statistic: # of shear peaks, regardless of whether or not they correspond to true bound objects
  as a function of height, redshift and angular size
  Kratochvil, Haiman, Hui & May (2010)
- Fundamental questions about “false” (non-cluster) peaks:
  1. How does N(peak) depend on cosmology ?
  2. What is the field-to-field variance ΔN(peak) ?
- Requires simulations

N-body Simulation Details

Kratochvil, Haiman, Hui & May (2010)

- pure DM (no baryons, neutrinos, or radiation)
- public code GADGET-2, modified to handle $w_0 \neq -1$
- fiducial ΛCDM cosmology from *WMAP*:
  $(w_0, \Omega_\Lambda, \Omega_m, H_0, \sigma_8, n) = (-1.0, 0.74, 0.26, 0.72, 0.79, 1.0)$
- fix *primordial* amplitude $\Delta^2_R = 2.41\times10^{-9}$ at $k = 0.002$ Mpc^{-1}
  (σ_8=0.79 vs. 0.75)
- two alternative cosmologies, differ only in w_0= -0.8 (or -1.2)
- 512^3 box, size $200h^{-1}$ Mpc, z_{in}=60, $M_{DM}=4.3\times10^9\ M_\odot$
- gravitational softening length ε_{Pl} = $7.5h^{-1}$ kpc
- output particle positions every $70h^{-1}$ comoving Mpc
- runs at NSF TeraGrid and IBM Blue Gene / Brookhaven

Simulating Weak Lensing Maps

- Ray-tracing
  - compute 2D potential (2048×2048) in each lens plane
  - implement algorithm to follow rays (Hamana & Mellier 2001)
  - compute shear (γ), convergence (κ) and reduced shear (μ)
- Mock "observational" parameters
  - gaussian 1-component shear noise from intrinsic ellipticity:

    $\sigma_\gamma = 0.15 + 0.035z$ (Song & Knox 2004)
  - $n_{gal} = 15$ arcmin^{-2} background galaxies, at $z_s = 1, 1.5$, and 2
  - smooth κ-map with 2D finite Gaussian 0.25 - 30 arcmin
  - use 3×3 deg^2 smoothed convergence maps
- Identifying peaks
  - find all local maxima, record their height κ_{peak}

Example

raw convergence map (3×3 deg^2 ; 2048×2048 pixels)

w=-1

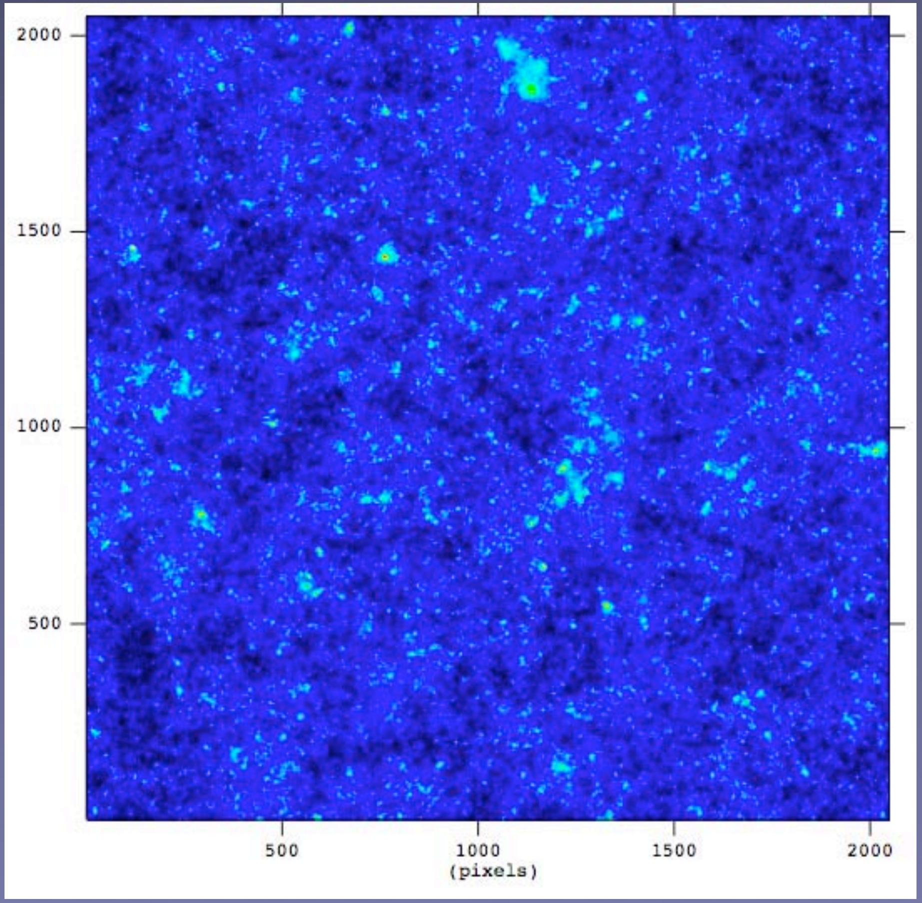

w=-0.8

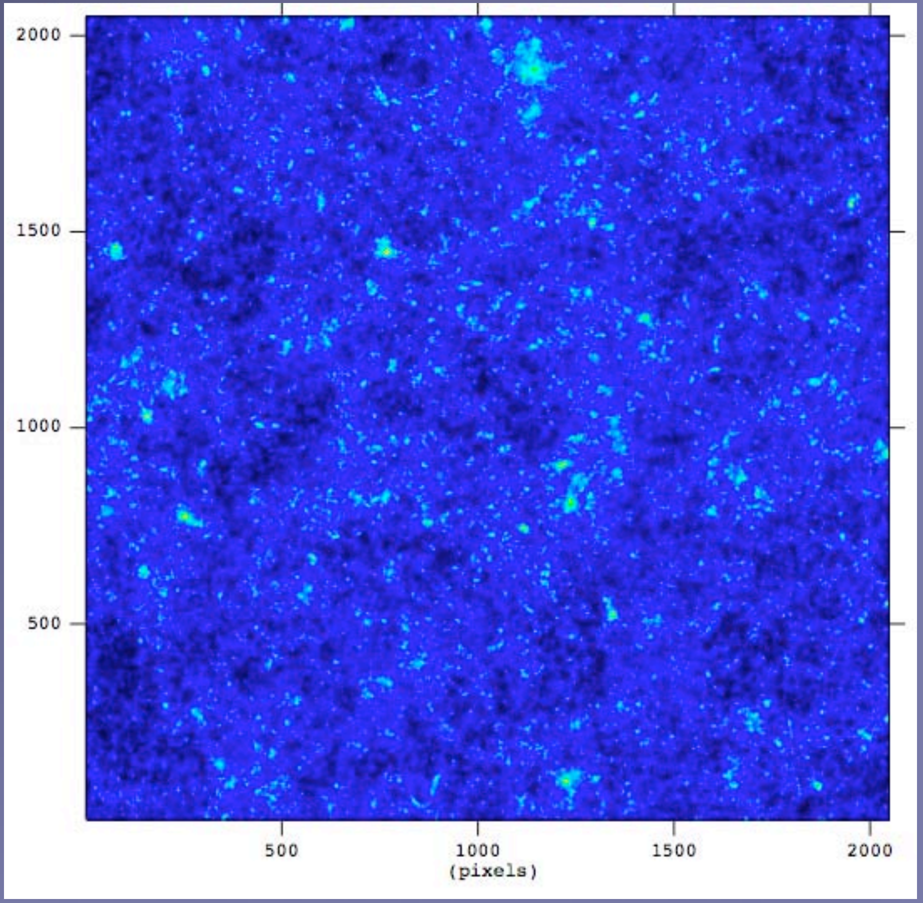

Example

convergence map with noise and 1-arcmin gaussian smoothing

w=-1

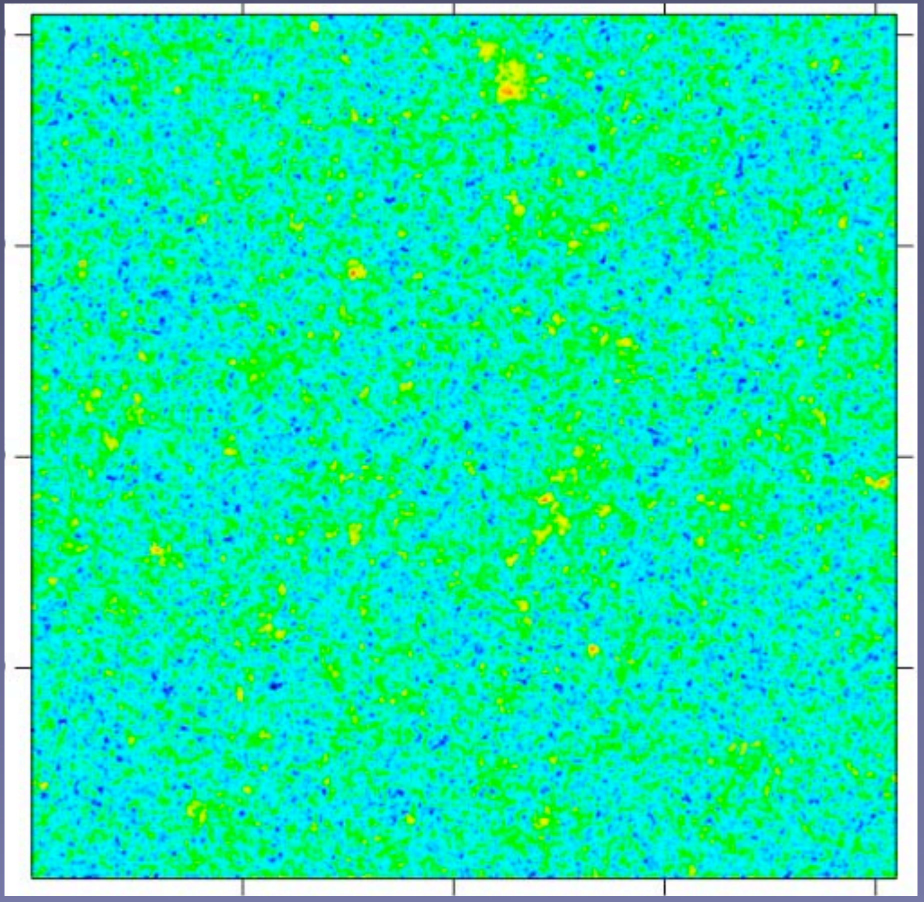

w=-0.8

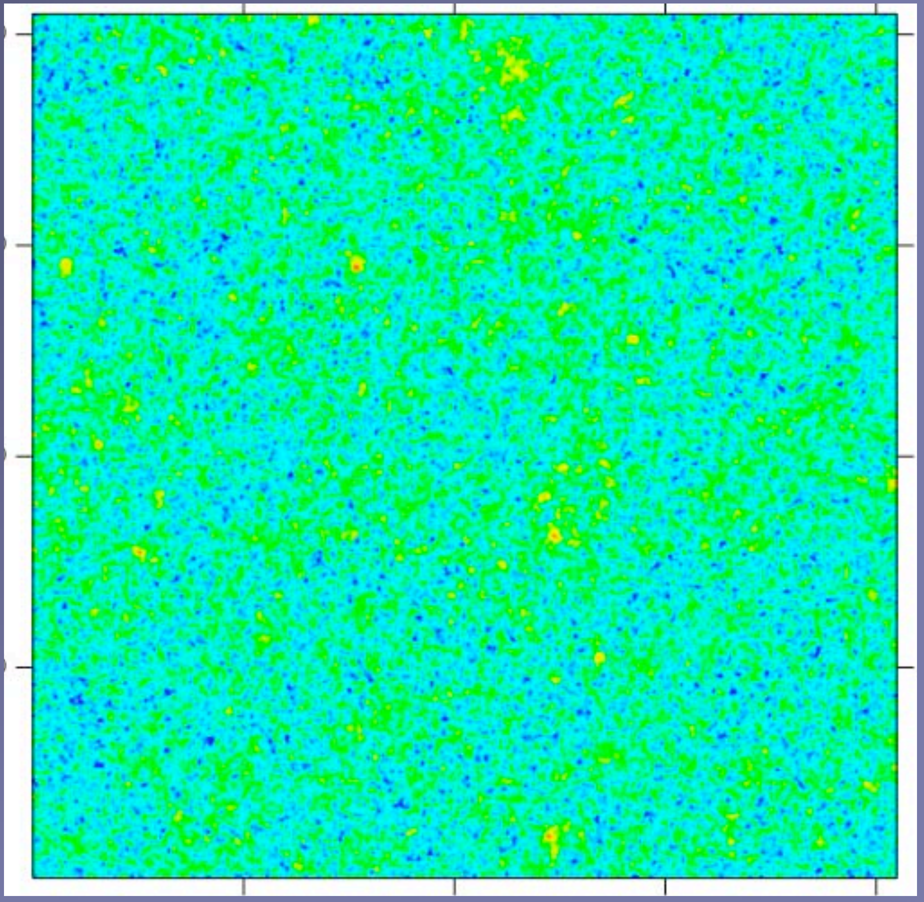

Basic Results

- 3×3 deg^2 field, smoothing with 1-arcmin, galaxies at z_s=2

- Expectations based on clusters with $\kappa_G \geq 4.5\sigma_\kappa$
  (Fang & Haiman 2007)
  N(clusters) = 150 ± 25 for *w*=-1
  N(clusters) = 103 ± 21 for *w*=-0.8
  ➔S/N≈*2σ mostly coming from change in* σ_8

- Total peak counts above same threshold [w/no noise]
  N(peaks) = 576 ± 86 [230 ± 42] for *w*=-1
  N(peaks) = 547 ± 85 [186 ± 37] for *w*=-0.8
  ➔S/N≈*0.3σ* : (i) smaller difference, (ii) larger variance

- Total peak counts (all peaks):
  N(peaks) = 11,622 ± 62 for *w*=-1
  N(peaks) = 11,562 ± 62 for *w*=-0.8

Statistical Methodology

- Covariance matrix for number of binned, tomographic peaks:

$$C^{m}_{i,j} \equiv \frac{1}{R-1}\sum_{r=1}^{R}\left[N^{m}_{i}(r)-\overline{N}^{m}_{i}\right]\left[N^{m}_{j}(r)-\overline{N}^{m}_{j}\right]$$

  - R=500 realizations in cosmology *m* (rotate/shift/slice box)
  - *i = 15 (height) x 3 (source redshift) = 45 bins*

- Compute "χ^2 " between test (*m*) and fiducial (*n*) cosmology:

$$\chi^{2;m,n}(r) \equiv \sum_{i,j=1}^{45}\left[N^{m}_{i}(r)-\overline{N}^{n}_{i}\right]\left[C^{n}_{i,j}\right]^{-1}\left[N^{m}_{j}(r)-\overline{N}^{n}_{j}\right]$$

- Compute likelihood at which cosmology *m* can be distinguished from cosmology *n*:
  - given by overlap between two distributions $\chi^{2;m,n}$ and $\chi^{2;n,n}$

Chi Square Distributions

3 redshift bins, 15 peak height bins, 0.5 arcmin smoothing

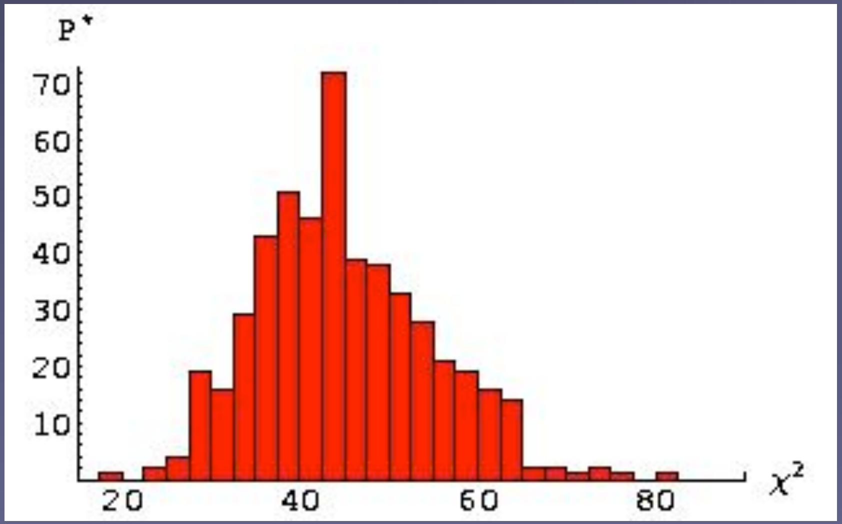

w = -1 versus w = -1

$\langle\chi^2\rangle$=44.89

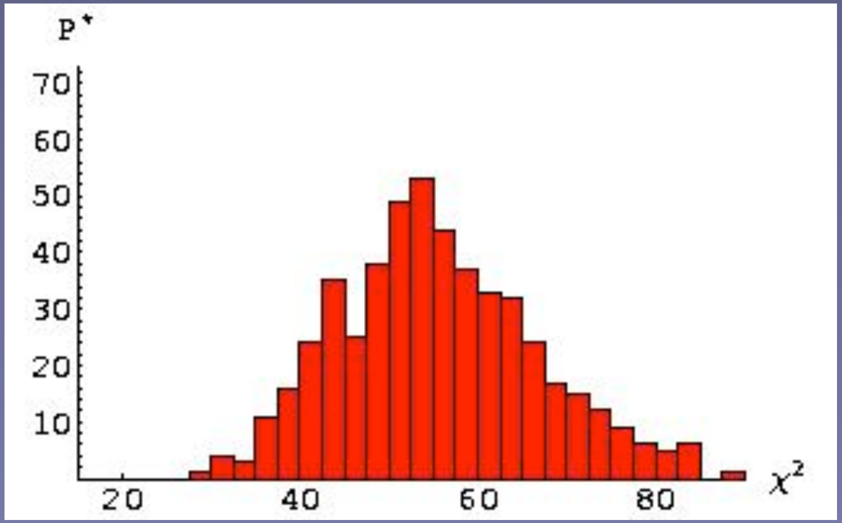

w=-0.8 versus w=-1

$\langle\chi^2\rangle$=55.51

$\rightarrow \Delta \langle\chi^2\rangle \approx 10$

or 85% confidence

Which peaks dominate constraints?

- smoothing with 0.5 arcmin, galaxies at z_s=2
- w=-1 more peaks at high+low ends (DE dominates later)
- w=-0.8 peaks are more sharply peaked
- medium height ($\kappa\approx$0.04, or 2σ) peaks dominate the total χ^2

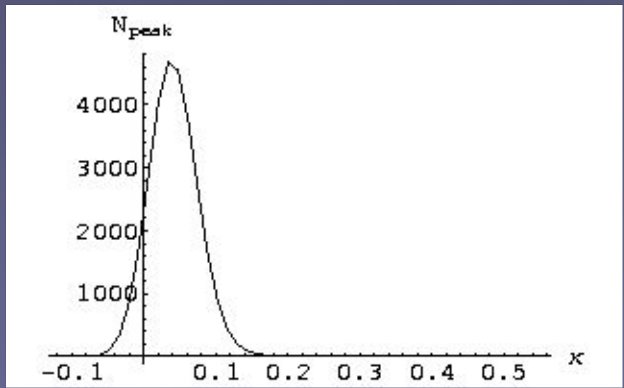

Total # of peaks

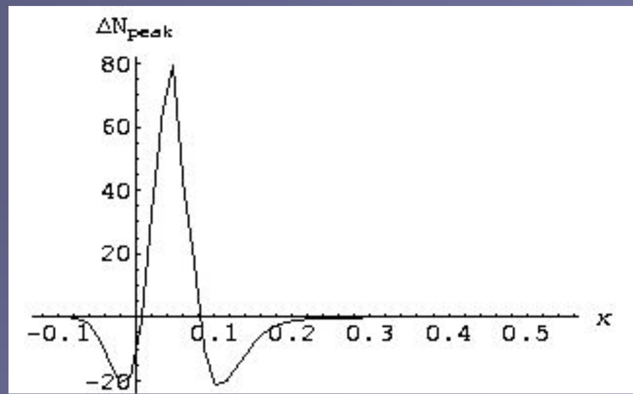

Difference in N_{peak}

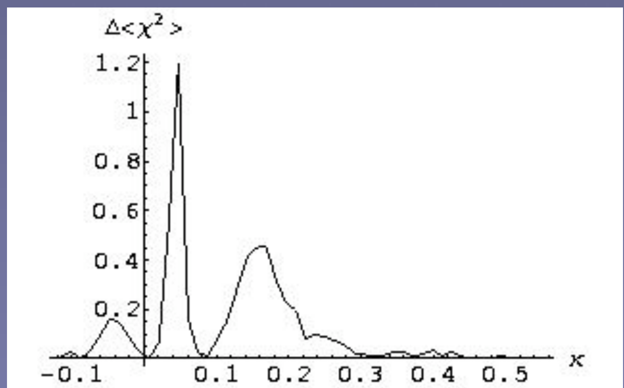

Contribution to χ^2

Results: statistical significance

- $w=-0.8$ distinguishable at 85% confidence from $w=-1.0$
  70% chance for 68% CL
  26% chance for 95% CL

- covariance has small effect overall (cuts high-χ^2 tail)

- co-adding several smoothing scales gives only modest (~10%) improvement over single best scale (~0.5 arcmin – smaller than best cluster case)

- scaling from $3\times3 = 9$ deg^2 to 20,000 deg^2 :
  rough guess:
  significance $\sqrt{(20{,}000/9)}=50$ times better
  1.5σ sensitivity to w_0 is $\Delta w_0 = 0.2/50 = 0.004$

Questions:

- what causes the medium-height peaks?
  - *(i) one ore more individual collapsed halos*
  - *(ii) mildly over-dense large-scale filaments*
  - *(iii) unvirialized 'half-collapsed' halos*
  - *(iv) galaxy shape noise*

- is the information in the medium-height peaks still complementary to the power spectrum?

  linear fluctuations in potential, or galaxy shape noise would both produce gaussian random fields

- parameter degeneracies?

  well known in the case of cluster counts; similar Ω_m-σ_8 *degeneracy found for peaks*

  (Dietrich & Hartlap 2010)

Suite of N-body Simulations

(Yang, Kratochvil, Wang, Lim, Haiman & May 2011, PRD, submitted)

- **80 new N-body runs; vary w, Ω_m, σ_8**
- **Higher resolution (4,096 x 4,096) density/potential planes**
- **15 gals/amin^2 at z_s=1 and z_s=2**

	σ_8	w	Ω_m	# of sims
Fiducial	0.798	-1.0	0.26	5
Control	0.798	-1.0	0.26	45
High-σ_8	0.850	-1.0	0.26	5
Low-σ_8	0.750	-1.0	0.26	5
High-w	0.798	-0.8	0.26	5
Low-w	0.798	-1.2	0.26	5
High-Ω_m	0.798	-1.0	0.29	5
Low-Ω_m	0.798	-1.0	0.23	5

TABLE I: *Cosmological parameters varied in each model. The universe is always assumed to be spatially flat ($\Omega_\Lambda + \Omega_m = 1$).*

Origin of Peaks

- **What causes peaks?**

  - identify halos, match them to peaks [use fiducial cosmology]

- **What drives the cosmology-dependence of peak counts?**

  - compare two different cosmologies (e.g. vary σ_8) with

  identical noise realization and (quasi) identical initial condition

Halo finding

- **AMIGA halo finder** (Knollmann & Knebe 2009)
- **[interesting cropped halos at box edges - make no difference]**
- **20% agreement in range $2\times10^{11} M_\odot < M < 3\times10^{14} M_\odot$**

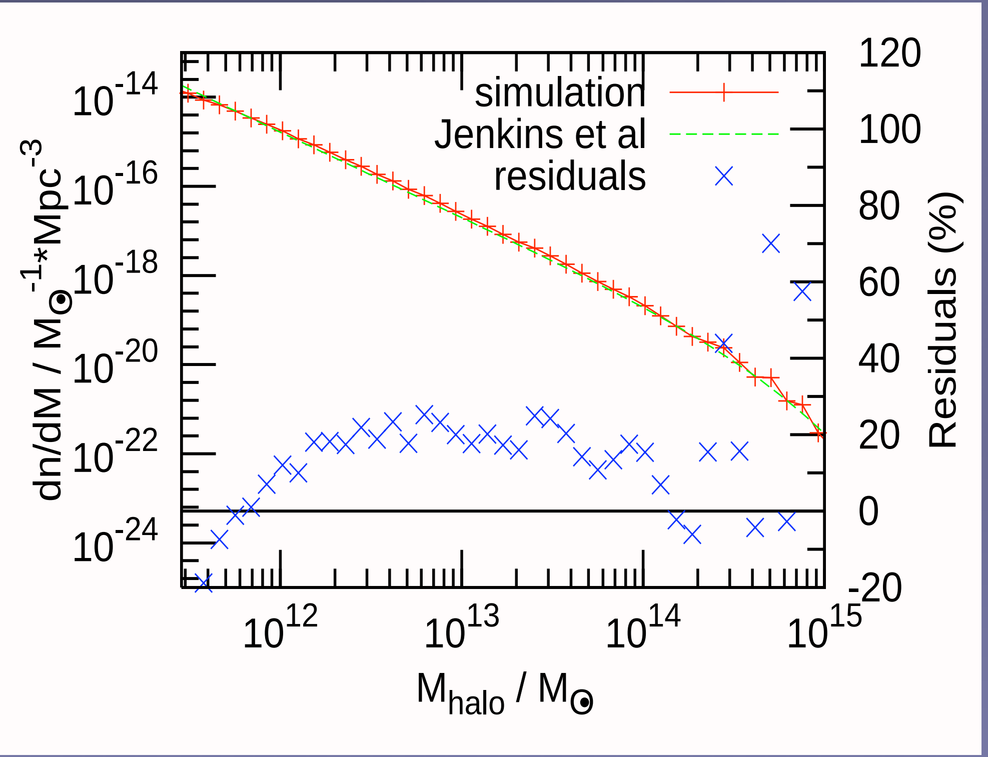

Halo contributions to convergence

- Assume spherical NFW halo with measured M_{vir}
- Compute $\kappa_{NFW}(\Phi, M_{vir})$ as a function of impact parameter Φ
- Compare to $\Delta\kappa$ when ray-tracing is repeated with halo removed

(fractional bias of -0.06; r.m.s. scatter of 0.15)

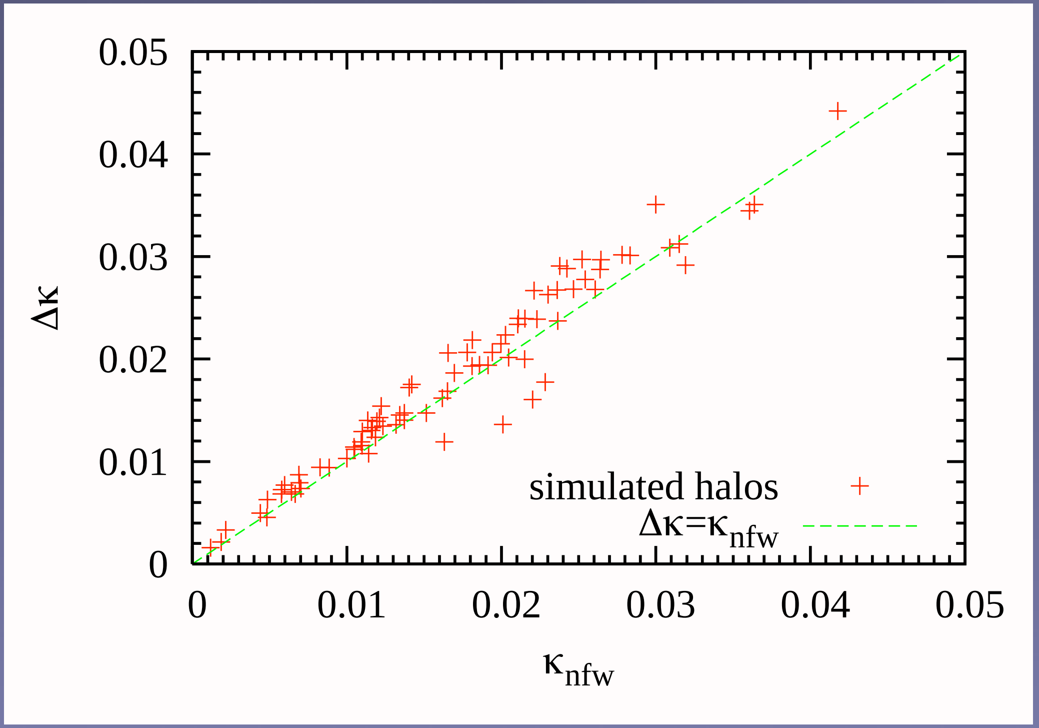

What causes peaks?

- identify halos, match them to peaks [use fiducial cosmology]

- use 50 noisy maps, 1 arcmin smoothing, 1.8 arcmin cone, z_s=2

- Peaks: 2,802 high ($\kappa > 4.8\sigma_{noise}$) 27,556 medium ($1.1\sigma_{noise} < \kappa < 1.6\sigma_{noise}$)

- Halos: 758 22,352

class	matching result	number of matches (high peaks)	(medium peaks)
i	halo ⇔ peak	526 (0.93)	2653 (4.7)
ii	halo with no paired peak	230 (0.41)	19609 (35)
iii	peak with no paired halo	2264 (4.0)	24709 (44)
iv	halo ⇒ peak	2 (0.0035)	90 (0.16)
v	halo ⇐ peak	12 (0.021)	194 (0.34)

10% of medium peaks have one-to-one match

90% of medium peaks/halos have no match

What causes peaks?

high peaks | **medium peaks**

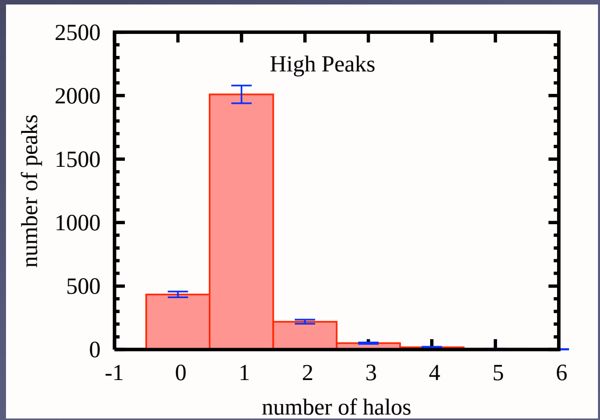

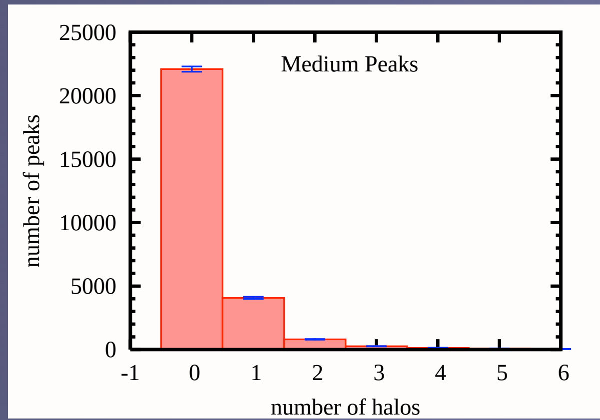

←noise or halo contributions

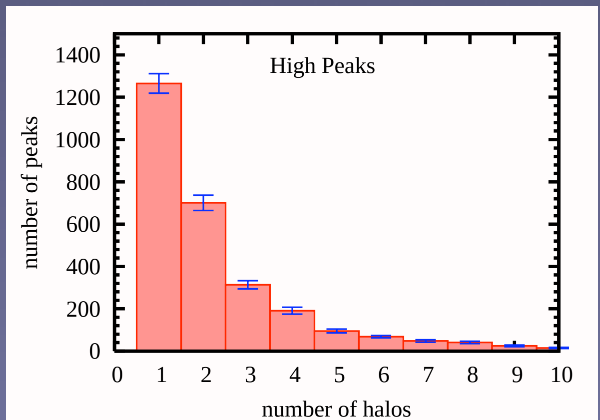

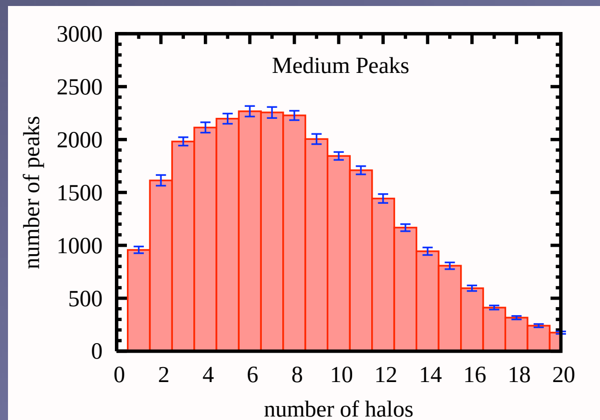

←halo only contributions

medium peaks are dominated by *noise* and the sum of 4-8 *halos* along the LOS

What drives cosmology-dependence?

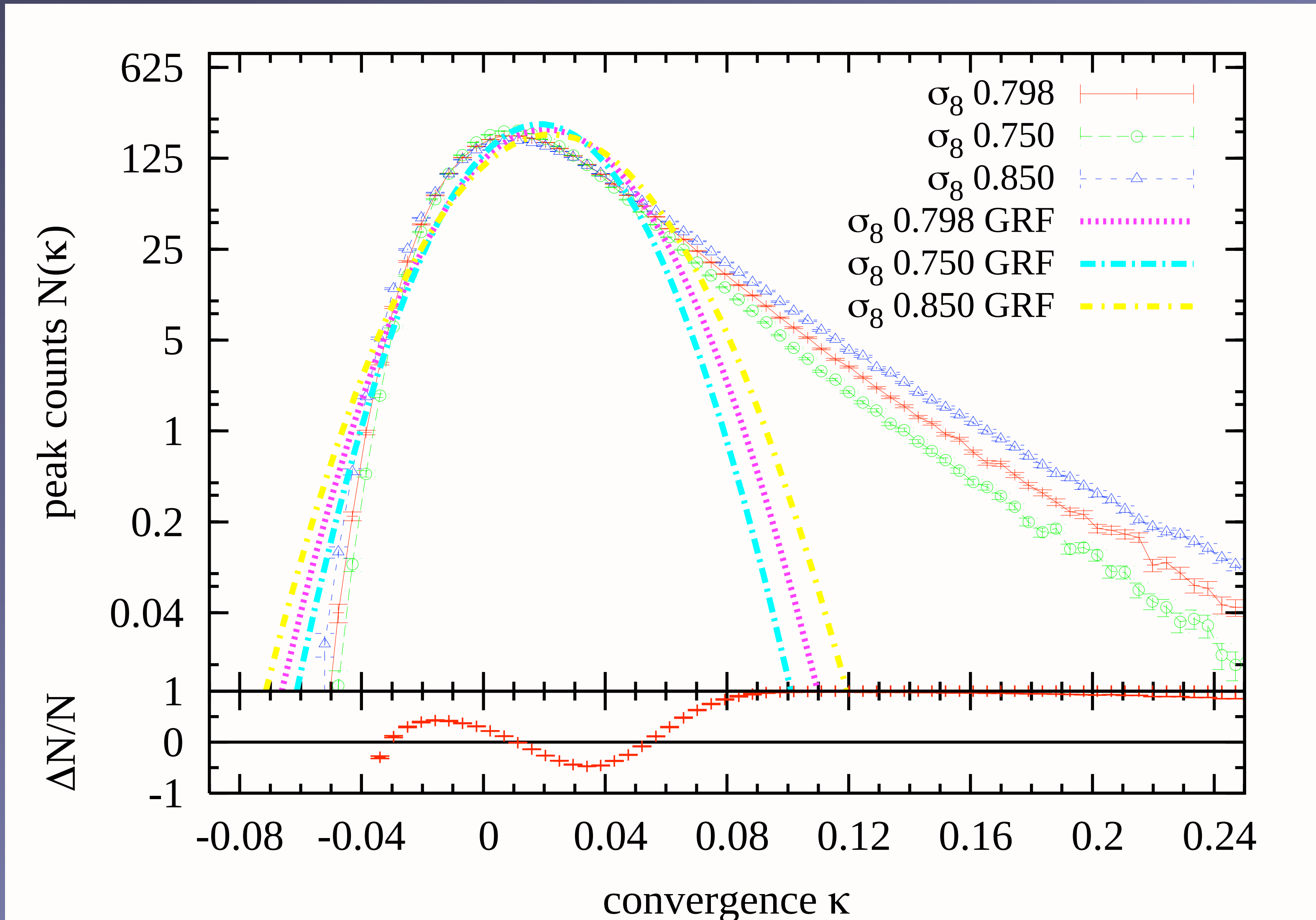

Peaks in a Gaussian Random Field:

- Mock maps = analytic prediction (Bond & Efstathiou 1987)
- Can compute covariance matrix numerically in GRF case

$$n_{\rm max}(\nu)d\nu = \frac{1}{2\pi\theta_*^2}\exp(-\nu^2/2)\frac{d\nu}{(2\pi)^{1/2}}G(\gamma,\gamma\nu) \quad (10)$$

where

$$G(\gamma,x_*) = (x_*^2-\gamma^2)[1-\frac{1}{2}{\rm erfc}\{\frac{x_*}{[2(1-\gamma^2)]^{1/2}}\}] + x_*(1-\gamma^2)\frac{\exp\{-x_*^2/[2(1-\gamma^2)]\}}{[2\pi(1-\gamma^2)]^{1/2}} + \frac{-x_*^2/(3-2\gamma^2)}{(3-2\gamma^2)^{1/2}} [1-\frac{1}{2}{\rm erfc}\{\frac{x_*}{[2(1-\gamma^2)(3-2\gamma^2)]^{1/2}}\}] \quad (11)$$

$$\gamma = \sigma_1^2/(\sigma_0\sigma_2) \quad (12)$$

$$\theta_* = \sqrt{2}\sigma_1/\sigma_2 \quad (13)$$

$$\sigma_p^2 = \int_0^\infty \frac{\ell d\ell}{2\pi}\ell^{2p}P_\ell = p!2^{2p}(-1)^p\frac{d^p\xi}{d(\theta^2)^p}(0), \quad (14)$$

$$n_{\rm pk} = (4\pi\sqrt{3})^{-1}\theta_*^{-2}. \quad (15)$$

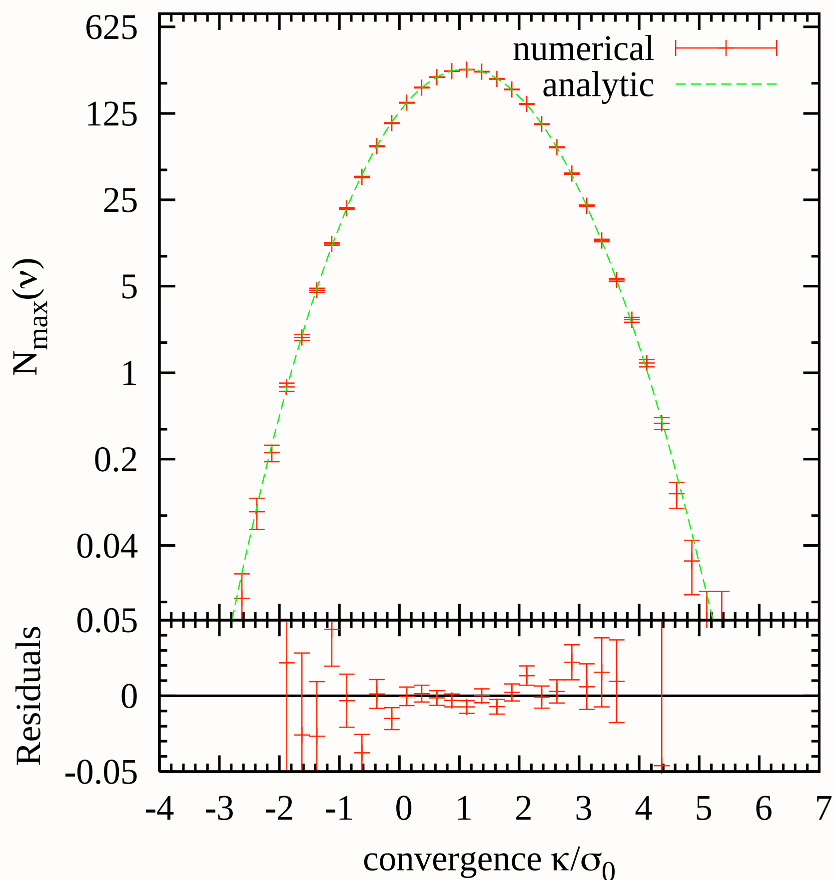

What drives cosmology-dependence?

- Why does number of medium peaks scale inversely with σ_8 ?

σ_8=0.80: 2,802 high 27,556 medium

σ_8=0.75: 1,987 high 29,097 medium

- Match individual peaks in the two cosmologies (via halos)

80-90% of high peaks have 1-1 correspondance (small κ bias)

55% of medium peaks → "fragile": sensitive to halo masses/locations

- Change in κ of individual peaks:

class	low-σ_8 → fiducial	fiducial → low-σ_8
exit to low κ	3303	3420
stay in bin	7683	7515
exit to high κ	5373	4408
total matched	16359	15343
lost (unmatched)	12738	12213

2/3rd of sensitivity due to "scatter" (net ~1000 peaks)

1/3rd to "destruction" (net ~500 peaks)

Cosmology Sensitivity

"NEVER show a Table in a talk slide!" - **David Spergel, Princeton, NJ, cca. 2002**

Cosmology Sensitivity

"NEVER show a Table in a talk slide!" - **David Spergel, Princeton, NJ, cca. 2002**

map type	cosmology pair	noiseless $\Delta\chi^2$ unscaled	noiseless $\Delta\chi^2$ scaled	noisy $\Delta\chi^2$ unscaled	noisy $\Delta\chi^2$ scaled
Sim	F and High-σ_8	5.16	0.46	5.89	4.29
GRF	F and High-σ_8	10.65	0.23	5.87	3.16
Sim	F and Low-σ_8	5.01	0.34	5.09	3.67
GRF	F and Low-σ_8	9.93	0.16	4.98	2.58
Sim	F and High-Ω_m	3.61	0.033	4.02	2.46
GRF	F and High-Ω_m	7.68	0.014	3.77	2.01
Sim	F and Low-Ω_m	4.39	0.053	4.44	2.56
GRF	F and Low-Ω_m	8.79	0.043	4.08	2.11
Sim	F and High-w	0.98	0.47	0.65	0.27
GRF	F and High-w	0.93	0.017	0.46	0.14
Sim	F and Low-w	0.44	0.27	0.36	0.16
GRF	F and Low-w	0.54	0.004	0.26	0.08

< $\Delta\chi^2$

from peak-counts between pairs of models

Cosmology Sensitivity

"NEVER show a Table in a talk slide!" - David Spergel, Princeton, NJ, cca. 2002

map type	cosmology pair	noiseless $\Delta\chi^2$ unscaled	noiseless $\Delta\chi^2$ scaled	noisy $\Delta\chi^2$ unscaled	noisy $\Delta\chi^2$ scaled
Sim	F and High-σ_8	5.16	0.46	5.89	4.29
GRF	F and High-σ_8	10.65	0.23	5.87	3.16
Sim	F and Low-σ_8	5.01	0.34	5.09	3.67
GRF	F and Low-σ_8	9.93	0.16	4.98	2.58
Sim	F and High-Ω_m	3.61	0.033	4.02	2.46
GRF	F and High-Ω_m	7.68	0.014	3.77	2.01
Sim	F and Low-Ω_m	4.39	0.053	4.44	2.56
GRF	F and Low-Ω_m	8.79	0.043	4.08	2.11
Sim	F and High-w	0.98	0.47	0.65	0.27
GRF	F and High-w	0.93	0.017	0.46	0.14
Sim	F and Low-w	0.44	0.27	0.36	0.16
GRF	F and Low-w	0.54	0.004	0.26	0.08

Raw sensitivity:

- direct sensitivity comparable to P_l

- sensitivity to w is ~10× weaker (NB no tomography)

Cosmology Sensitivity

"NEVER show a Table in a talk slide!" - David Spergel, Princeton, NJ, cca. 2002

map type	cosmology pair	noiseless $\Delta\chi^2$ unscaled	noiseless $\Delta\chi^2$ scaled	noisy $\Delta\chi^2$ unscaled	noisy $\Delta\chi^2$ scaled
Sim	F and High-σ_8	5.16	0.46	5.89	4.29
GRF	F and High-σ_8	10.65	0.23	5.87	3.16
Sim	F and Low-σ_8	5.01	0.34	5.09	3.67
GRF	F and Low-σ_8	9.93	0.16	4.98	2.58
Sim	F and High-Ω_m	3.61	0.033	4.02	2.46
GRF	F and High-Ω_m	7.68	0.014	3.77	2.01
Sim	F and Low-Ω_m	4.39	0.053	4.44	2.56
GRF	F and Low-Ω_m	8.79	0.043	4.08	2.11
Sim	F and High-w	0.98	0.47	0.65	0.27
GRF	F and High-w	0.93	0.017	0.46	0.14
Sim	F and Low-w	0.44	0.27	0.36	0.16
GRF	F and Low-w	0.54	0.004	0.26	0.08

How much of the Information is in σ_κ?:

- not most of it!

- note: almost all of the info in the *noiseless* maps is in σ_κ → "non-linear interaction" between signal and noise

Convergence power spectrum

- Noise-free, unsmoothed maps, using z_s=2
- Theoretical prediction based on NL matter power spectrum

(Nicaea; Kilbinger et al. 2009)

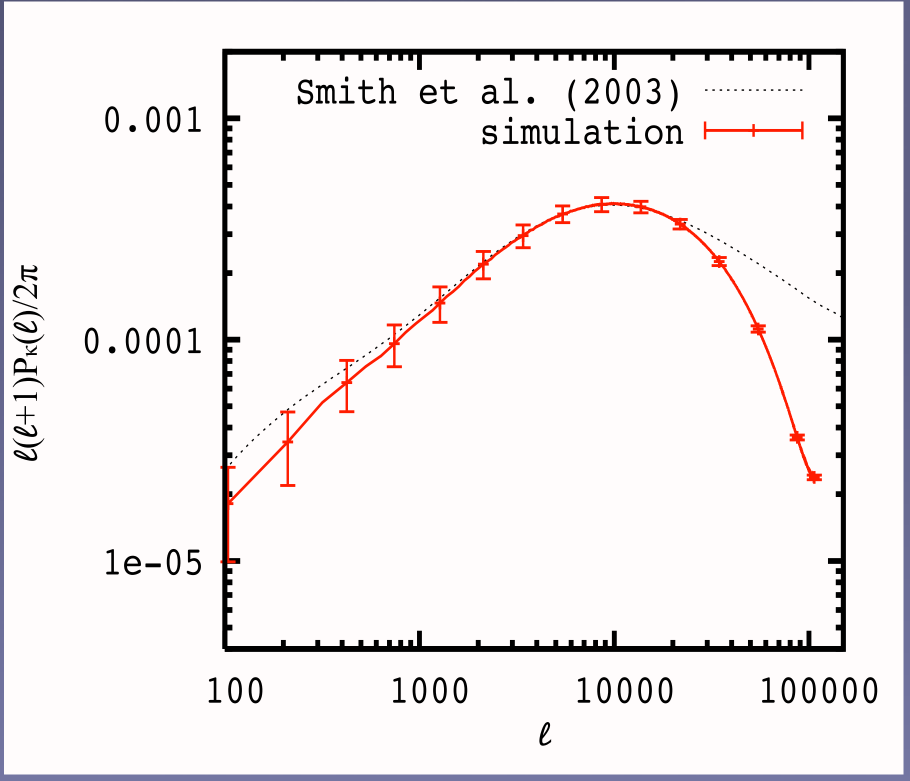

- Agreement in the range

  400 < *l* < 30,000

Is there info beyond power spectrum?

Treat $P_i = l(l+1)P(l)$ in 5 bins $100 < l < 20{,}000$ as 5 additional observables, compute $C_{ij} = \langle (P_i - \langle P_i \rangle)(P_j - \langle P_j \rangle) \rangle$

and cross-terms $C_{ij} = \langle (P_i - \langle P_i \rangle)(N_j - \langle N_j \rangle) \rangle$

observable type	cosmology	noiseless $\Delta\chi^2$	noisy $\Delta\chi^2$
Peak Counts ($\Delta\chi^2_N$)	Fiducial	5.16	5.89
Power Spectrum ($\Delta\chi^2_P$)	and	17.06	8.12
Combination ($\Delta\chi^2_{NP}$)	High-σ_8	37.07	16.36
$\Delta\chi^2_{NP}/(\Delta\chi^2_N + \Delta\chi^2_P)$		1.67	1.17
Peak Counts ($\Delta\chi^2_N$)	Fiducial	5.01	5.09
Power Spectrum ($\Delta\chi^2_P$)	and	13.03	5.76
Combination ($\Delta\chi^2_{NP}$)	Low-σ_8	26.79	11.87
$\Delta\chi^2_{NP}/(\Delta\chi^2_N + \Delta\chi^2_P)$		1.49	1.09
Peak Counts ($\Delta\chi^2_N$)	Fiducial	3.61	4.02
Power Spectrum ($\Delta\chi^2_P$)	and	17.69	6.15
Combination ($\Delta\chi^2_{NP}$)	High-Ω_m	32.42	11.65
$\Delta\chi^2_{NP}/(\Delta\chi^2_N + \Delta\chi^2_P)$		1.52	1.15
Peak Counts ($\Delta\chi^2_N$)	Fiducial	4.39	4.44
Power Spectrum ($\Delta\chi^2_P$)	and	16.49	5.61
Combination ($\Delta\chi^2_{NP}$)	Low-Ω_m	29.47	10.94
$\Delta\chi^2_{NP}/(\Delta\chi^2_N + \Delta\chi^2_P)$		1.41	1.09
Peak Counts ($\Delta\chi^2_N$)	Fiducial	0.98	0.65
Power Spectrum ($\Delta\chi^2_P$)	and	0.92	0.29
Combination ($\Delta\chi^2_{NP}$)	High-w	2.79	0.84
$\Delta\chi^2_{NP}/(\Delta\chi^2_N + \Delta\chi^2_P)$		1.46	0.90
Peak Counts ($\Delta\chi^2_N$)	Fiducial	0.44	0.36
Power Spectrum ($\Delta\chi^2_P$)	and	0.64	0.19
Combination ($\Delta\chi^2_{NP}$)	Low-w	1.69	0.51
$\Delta\chi^2_{NP}/(\Delta\chi^2_N + \Delta\chi^2_P)$		1.57	0.92

- **Raw sensitivities of N and P are comparable**
- **P(l) degraded more by noise**
  noise adds no signal δP
- **Synergy from combination:**
  cosmology-induced changes (δN, δP) do not obey correlations
  $\langle \Delta N \Delta P \rangle \neq 0$

Marginalized Errors

- *Fisher matrix – use backward/forward finite difference*
- *Use 15 κ-bins; scale errors by angle sqrt(20,000/12)~50*

- **Tomography improves marginalized errors by factor of ~two**
  redshift-dependent parameter-sensitivities are non-degenerate

- **Factor of ~2 from adding peak counts to power spectrum**
  counts contain information beyond P(l)

marginalized error	σ_8	w	Ω_m
z2	0.0065	0.030	0.0057
z1	0.0078	0.036	0.0057
z2+z1	0.0024	0.018	0.0022
Power Spectrum ($z_s = 2$)	0.0047	0.026	0.0028
z2+Power Spectrum	0.0026	0.012	0.0019
z1+Power Spectrum	0.0037	0.020	0.0026
tomography combined	0.0012	0.0096	0.0010
combined/(z2+Power Spectrum)	0.47	0.79	0.52

Minkowski Functionals

- One of several general topological measures of isodensity surfaces (in 3D) or contours (2D)
  - an alternative probe of non-Gaussianity

    Gott et al. (1982)

- Examples of previous applications
  - genus in 3-D galaxy distribution in SDSS
  - 2D Minkowski Functionals in CMB: search for primordial non-Gaussianity (f_{NL} limits similar to bispectrum)
  - fractional-area $P(>\kappa_{th})$ in WL – a.k.a. V_0, one of 3 MFs

    Wang et al. (2009)
  - genus in WL maps: V_2 (OCDM vs SCDM; Matsubara & Jain 2001)

- Robustly measurable in data and in our set of simulations

Minkowski Functionals

(Kratochvil, Lim, Wang, Haiman, May & Huffenberger 2011, in prep)

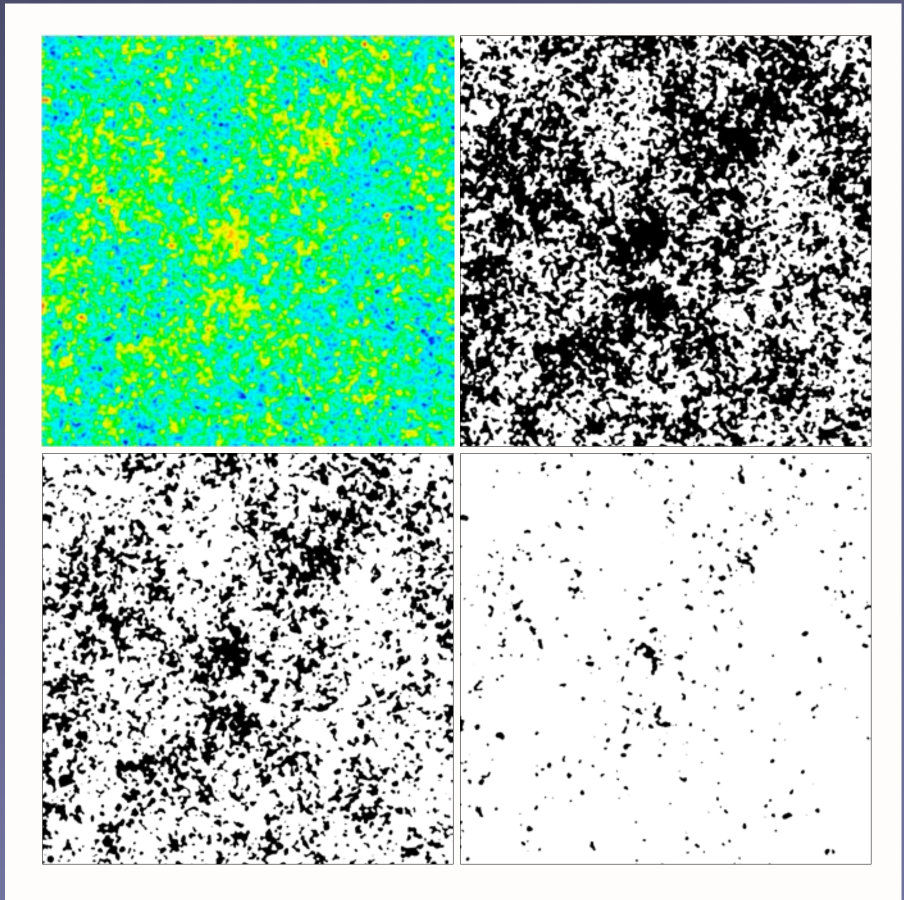

contours as a function of the threshold κ_{th}

- V_0: *area* above κ_{th}
- V_1: contour *boundary length*
- V_2: *Euler characteristic* #connected regions above minus #below κ_{th}

Any functional that is additive, translation-invariant, and continuous, is a linear combination of V_1, V_2, and V_3.

Minkowski Functionals

Depend on threshold, and on 1st and 2nd derivatives of κ(x,y)

$$V_0(\nu) = \int_{\mathbf{R}^2} \Theta(\kappa - \nu)\ da$$

$$V_1(\nu) = \frac{1}{4}\int_{\mathbf{R}^2} |\nabla\kappa|\delta(\kappa - \nu)\ da$$

$$V_1(\nu) = \frac{1}{2\pi}\int_{\mathbf{R}^2} |\nabla\kappa|\delta(\kappa - \nu)K\ da$$

Measure in simulations using finite difference

$$V_0(\nu) = \int_{\mathbf{R}^2} \Theta(\kappa(\mathbf{x}) - \nu)\ da \tag{8}$$

$$V_1(\nu) = \int_{\mathbf{R}^2} \delta(\kappa(\mathbf{x}) - \nu)\sqrt{\kappa_x^2 + \kappa_y^2}\ da \tag{9}$$

$$V_2(\nu) = \int_{\mathbf{R}^2} \delta(\kappa(\mathbf{x}) - \nu)\frac{2\kappa_x\kappa_y\kappa_{xy} - \kappa_x^2\kappa_{yy} - \kappa_y^2\kappa_{xx}}{\kappa_x^2 + \kappa_y^2}\ da \tag{10}$$

Minkowski Functionals in a GRF

Calculable analytically

$$V_0^{\mathrm{GRF}}(\nu) = \frac{1}{2}\left[1 - \mathrm{Erf}\left(\frac{\nu-\mu}{\sqrt{2}\sigma_0}\right)\right]$$

$$V_1^{\mathrm{GRF}}(\nu) = \frac{1}{8\sqrt{2}}\frac{\sigma_1}{\sigma_0}\exp\left(-\frac{(\nu-\mu)^2}{2\sigma_0^2}\right)$$

$$V_2^{\mathrm{GRF}}(\nu) = \frac{\nu-\mu}{4\sqrt{2}}\frac{\sigma_1^2}{\sigma_0^3}\exp\left(-\frac{(\nu-\mu)^2}{2\sigma_0^2}\right)$$

where μ is the mean, and

$$\sigma_0 = \sqrt{\langle\kappa^2\rangle - \mu^2}$$

is the standard deviation while

$$\sigma_1 = \sqrt{\langle\kappa_x^2 + \kappa_y^2\rangle}$$

is its first moment.

Fractional Area of "Hot Spots"

Wang, Haiman & May (2009)

- A simple statistic: one-point function of convergence
  i.e. fraction of sky above a fixed threshold $\kappa > \kappa_T = \nu\sigma_N$
  "analytically" calculable, analogous to mass function:

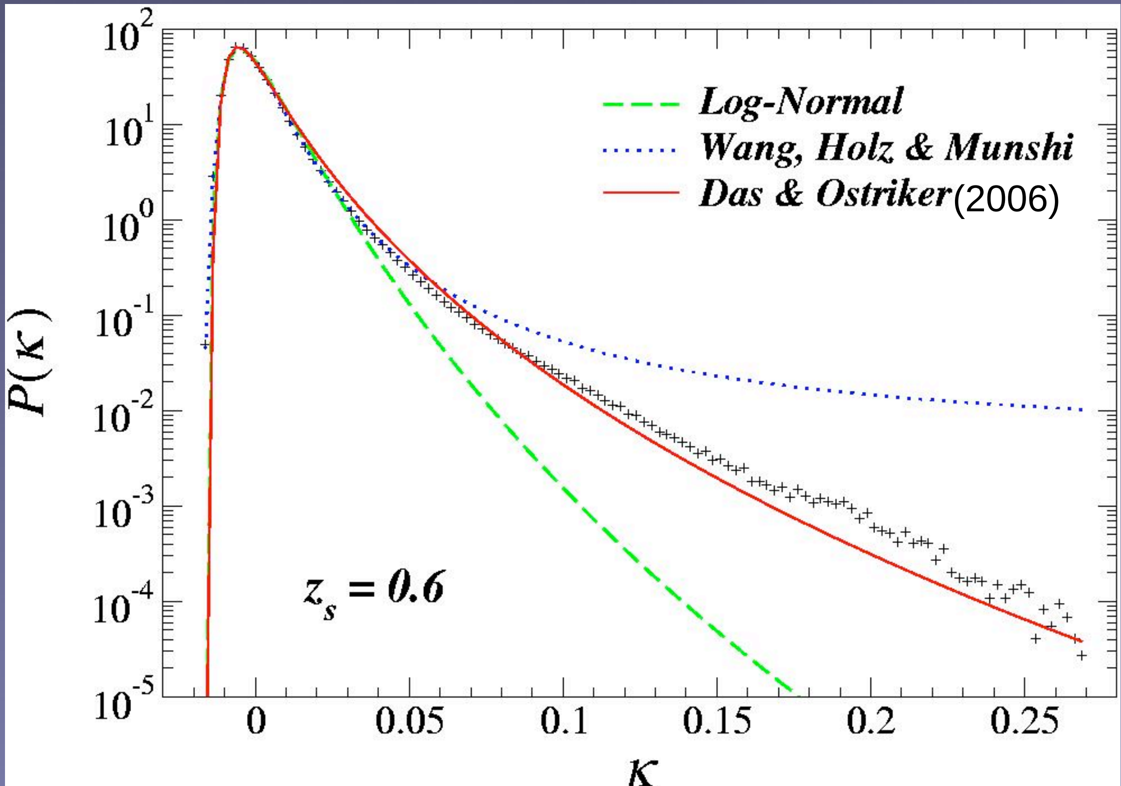

cosmology dependence only through $\langle\kappa^2\rangle$ and κ_{min}

$F = \int_{\nu\sigma} P(\kappa) d\kappa$

Simulations by M.White (2005)

Minkowski Functionals

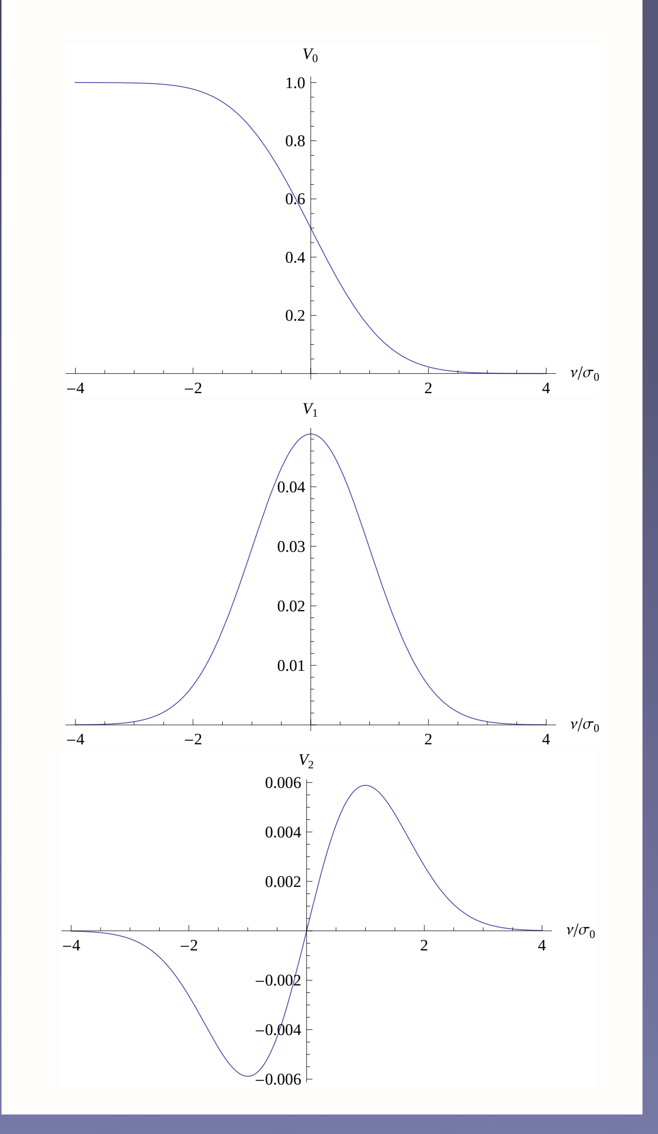

- **V_0: *area* above κ_{th}**
- **V_1: contour *boundary length***
- **V_2: *Euler characteristic* genus: #connected regions above minus #below κ_{th}**

Minkowski Functionals

$V_i(\mathrm{fid})$ $\Delta V_i = V_i - V_i(\mathrm{fid})$

$z_s = 2$

$\theta = 1'$

$n = 15/\mathrm{amin}^2$

1,000 maps

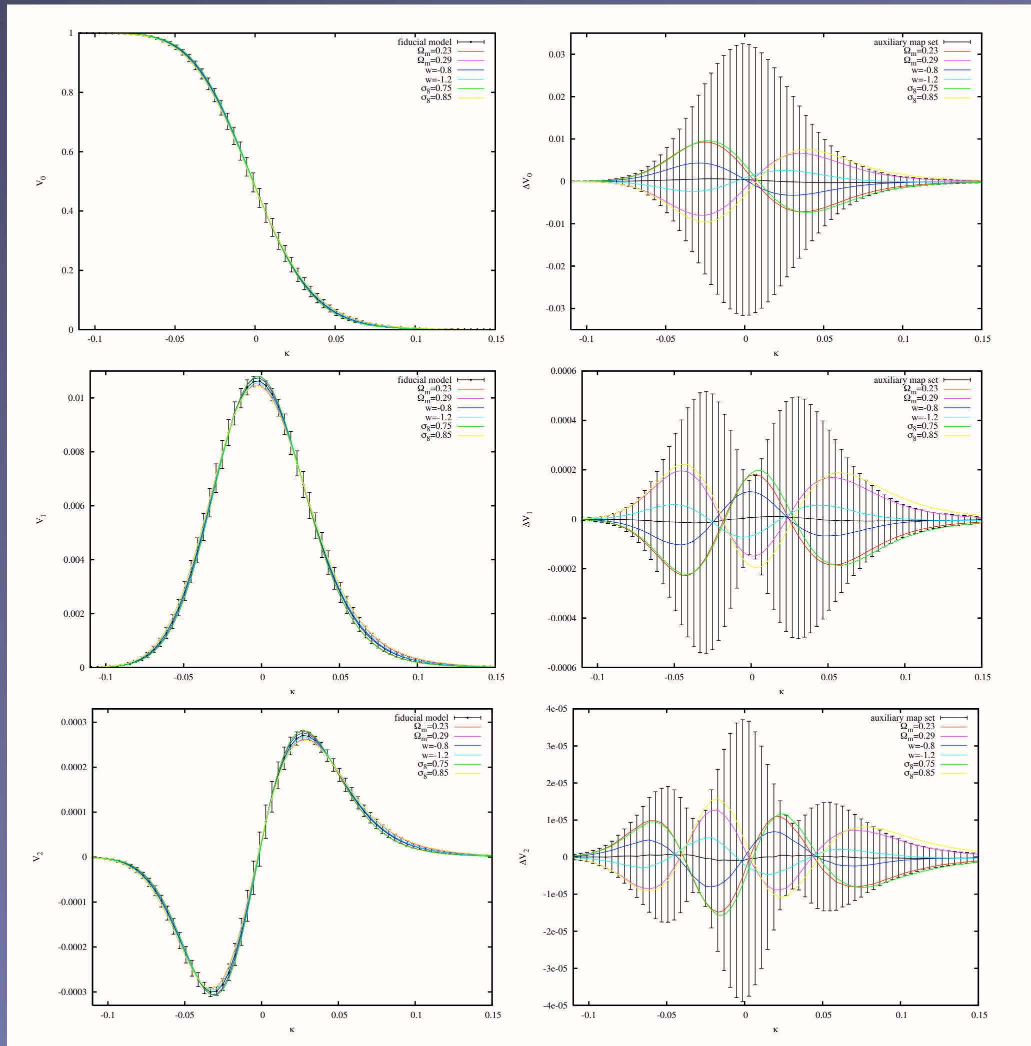

V_0

V_1

V_2

Marginalized Errors

- **MFs deliver factor of 1.5-2 tighter errors than power spectrum**
  (V_1 best individual sensitivity; V_1 ,V_2 have comparable errors)
- **Monte-Carlo errors – good agreement with Fisher matrix**
  (slight asymmetry in error bars)
- **Backward vs Forward derivatives**
  (small asymmetry)

	$\Delta\Omega_m$	Δw	$\Delta\sigma_8$
$z_s = 2$, $\theta_G = 1'$			
V_0	-0.00322 (-0.00317) 0.00319 (0.00322)	-0.0151 (-0.0158) 0.0154 (0.016)	-0.00391 (-0.00357) 0.00395 (0.00345)
V_1	-0.0019 (-0.00141) 0.00192 (0.00147)	-0.0113 (-0.00781) 0.0108 (0.00803)	-0.0026 (-0.002) 0.00265 (0.00193)
V_2	-0.00192 (-0.00155) 0.00183 (0.00151)	-0.0123 (-0.00735) 0.0118 (0.00752)	-0.00253 (-0.00206) 0.00257 (0.00202)
PS	-0.00252 (-0.00178) 0.00253 (0.00175)	-0.0183 (-0.0134) 0.0174 (0.0134)	-0.00421 (-0.0029) 0.00427 (0.00294)
MFs	-0.00162 (-0.00129) 0.00162 (0.00126)	-0.00896 (-0.00659) 0.00929 (0.00651)	-0.00225 (-0.00168) 0.00216 (0.00176)

Marginalized Errors (preliminary!)

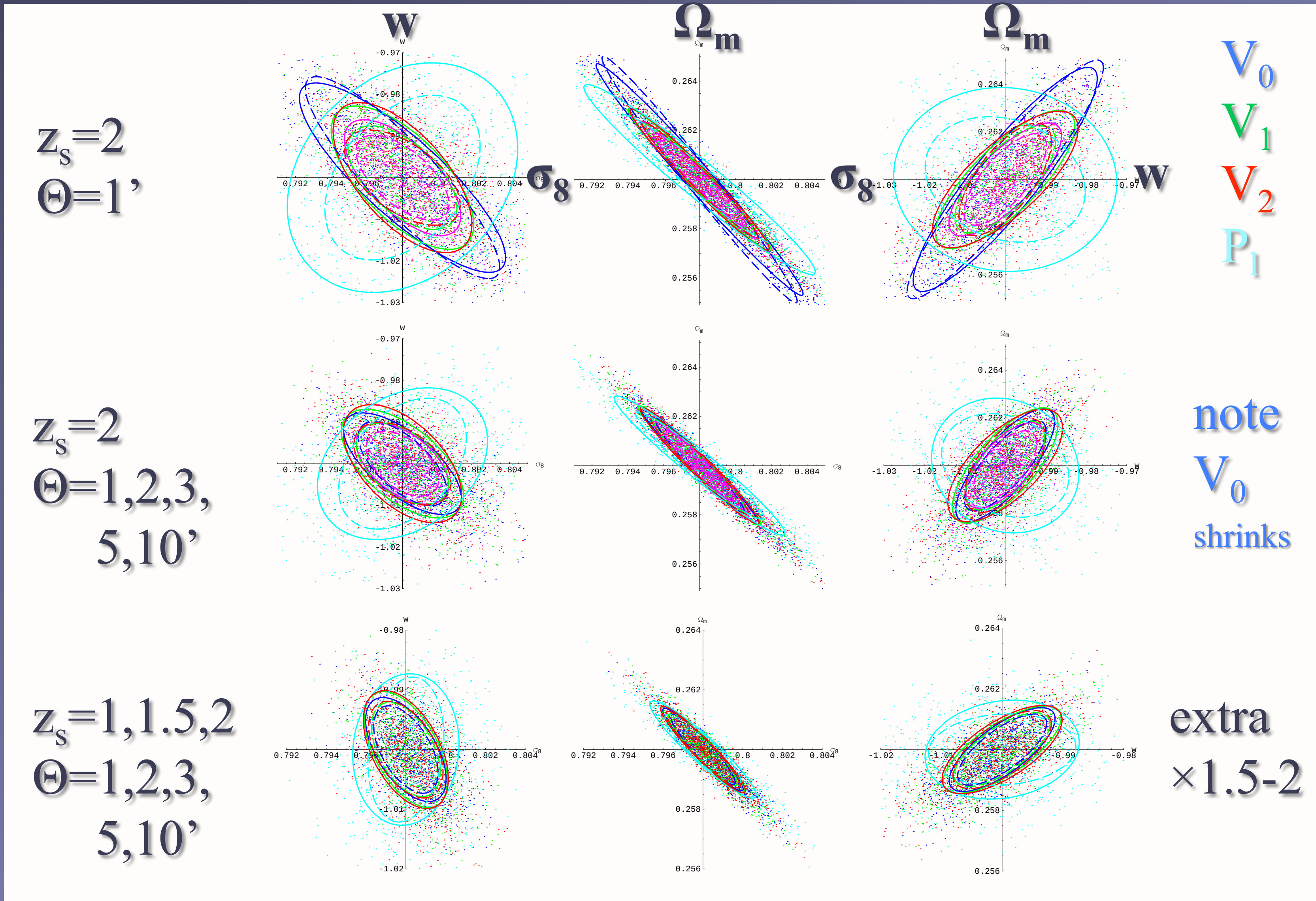

Conclusions

- Peak counts and MFs deliver constraints on Ω_m, w, σ_8 comparable or tighter than the power spectrum
- This information is new: from non-linear, non-Gaussian regime, complementary to the power spectrum
- Peaks: most info is in medium peaks, from halo projections
- MFs: V_1 most sensitive, V_2 comparable for marginalized errors; V_0 comparable w/multiple smoothing scales combined